Available online at www.sciencedirect.com
SCIENCE DIRECT®
Planetary and Space Science 53 (2005) 275–281
Planetary and Space Science
www.elsevier.com/locate/pss

Source positions of energetic particles responsible for the fine dispersion structures: numerical simulation results

V.N. Lutsenko[a,*], I.P. Kirpichev[a], T.V. Grechko[a], D. Delcourt[b]

[a]Space Research Institute, Russian Academy of Sciences, Profsoyuznaya 84/32, 117997 Moscow, Russian Federation
[b]Centre d'etude des Environnements Terrestre et Planetaires (CETP), CNRS — Observatoire de Saint-Maur, France

Accepted 12 September 2004

Abstract

More than 400 events with fine dispersion structures (FDS) in energetic particle spectra were observed in DOK-2 experiments onboard Interball-1 and -2 spacecraft in auroral regions. The discovery of these structures was possible due to high energy resolution of the spectrometer used. In previous studies we have suggested that these structures result from a gradient-curvature drift of ions and electrons after their impulsive injection (acceleration) in the nightside magnetosphere. The analysis of dispersion structures allowed us to find the injection time with an accuracy up to 10 s. In this work, numerical particle motion simulation backward in time is carried out in order to find source positions for two FDS events. In both cases the positions are found in the evening–midnight sector of MLT. The comparison of the simulation results with observations of particles that experience several turns around the Earth, explains some peculiarities of the FDS structures and may open new possibilities to check magnetic field models.

Keywords: Energetic particles; Dispersion structures; Magnetosphere; Substorms; Particle acceleration; Magnetic field models; Particle motion simulation

1. Introduction

Dispersion effects in energetic particle fluxes were already investigated in several works based on observations at geosynchronous orbit (Belian et al., 1984; Birn et al., 1996), on the AMPTE/CCE (Anderson and Takahashi, 2000), and on the Polar in the cusp (Karra and Fritz, 1999). In DOK-2 experiments onboard Interball-1 and -2 satellites, we observed more than 400 events that exhibit narrow lines in ion and electron spectra moving smoothly from high to low energies (Lutsenko et al., 2000, 2002). The energy resolution of the DOK-2 spectrometer was 6–10 times higher than that of other similar experiments. With its two pairs of telescopes (angles between telescope axis and the solar direction were 180 and 60 or 80 °) DOK-2 measured all ion spectra in a range $E = 20$–800 keV with an energy resolution of 8 keV (56 channels) and electron spectra in a range $E = 25$–400 keV with an energy resolution of 6 keV (55 channels) (Lutsenko et al., 1998). The spectrum accumulation time (time resolution) was variable and in auroral regions was usually about 10–15 s. So these high energy and time resolution data may provide new insights into the nature and properties of this phenomenon. We have shown earlier (Lutsenko et al., 2000) that these lines (we call them fine dispersion structures (FDS)), which were observed in $\sim 20\%$ of intersections by the Interball satellites of auroral and neighbouring regions, result from impulsive injection of protons, alpha-particles and electrons of all energies in the night side magnetosphere, followed by gradient-curvature drift around the Earth. The energy range for

*Corresponding author. Tel.: +7 095 333 2000; fax: +7 095 310 7023.
E-mail address: vlutsenk@iki.rssi.ru (V.N. Lutsenko).

0032-0633/$ - see front matter © 2004 Elsevier Ltd. All rights reserved.
doi:10.1016/j.pss.2004.09.053

FDS is from ~ 60 to 600 keV, so this phenomenon may differ from hot plasma injections during substorms (see, e.g., McIlwain, 1974). Analysis of FDS data allows us to estimate the injection time $T0$ with an accuracy of 10–30 s (from q/E vs. time plots) as well as the injection duration and longitudinal source extent (from the spectral line width). As for the location of the injection region, it can be found, in principle, via backward simulation of particle trajectories in model magnetic field from observation site and time T to time $T0$. We present here preliminary results of such simulations, which also allow us to compare the observed drift period with predictions from different magnetic field models for outer magnetosphere and accordingly to test these models.

2. Estimation of the injection duration and dimension of the injection region

Fig. 1 shows an example of ion spectra with dispersion lines. According to FDS nature mentioned above the full-width at half-maximum (FWHM) of the FDS line ΔE consists of four main parts, the first two of them being instrumental, namely:

1. a spectrometer resolution $\Delta E1$,
2. $\Delta E2$, depending on the spectrum accumulation time ΔT_{sp},
   $\Delta E2 = \Delta T_{sp} \times (dE/dt)$,
3. $\Delta E3$, depending on the spread in start times and relating to the injection duration ΔT_{inj} : $\Delta E3 = \Delta T_{inj} \times (dE/dt)$,

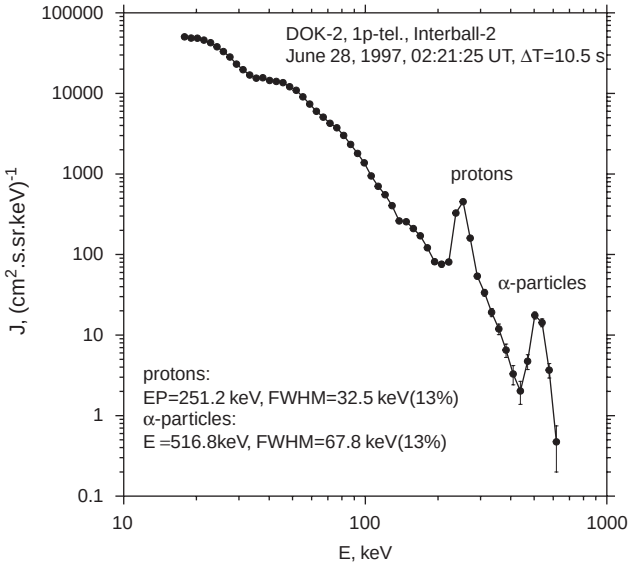

Fig. 1. Example of ion spectrum with FDS lines observed in the auroral region.

4. $\Delta E4$, depending on the spread in initial longitudinal (or MLT) positions φ and relating to the injection region dimension $\Delta\varphi$,
   $\Delta E4 = \Delta\varphi/(d\varphi/dt) \times (dE/dt)$.

Here (dE/dt) and $(d\varphi/dt)$ denote the line energy change and drift velocities. One would expect the line width to depend also upon the spread of initial pitch angles, but our simulations reveal that except trajectories very close to the magnetopause the dependence on pitch angle is rather weak (for the spacecraft positions at MLAT = 50–60°and in the DOK-2 observations pitch angle range).

As we know the total FWHM ΔE (see Fig. 1) and the first two of its constituents, we can estimate the common contribution of the last two. For the spectrum in Fig. 1, one has $\Delta E = 32.5$ keV, $\Delta E1 = 8$ keV, $\Delta T_{sp} = 10.5$ s, $dE/dt = -0.323$ keV/s which gives $\Delta E2 = 3.4$ keV. The residual $32.5 - 8 - 3.4 = 21.1$ keV should correspond to a joint deposition of spreads in start times ΔT_{inj} and start MLT positions $\Delta\varphi$, which we suppose to be independent random variables. The residual peak width corresponds to a time interval: $21.1/(dE/dt) = 65.3$ s. The $d\varphi/dt$ was estimated using simulations in model magnetic fields and found to be about 0.02 h/s. So for mean square deviations ΔT_{inj} and $\Delta\varphi$ we obtain: $\Delta T_{inj}^2 + (\Delta\varphi/(d\varphi/dt))^2 = (65.3)^2$, which yields the following upper limits: $\Delta T_{inj} < 65.3$ s, $\Delta\varphi < 1.3$ h MLT.

3. Simulation of ions and electrons motion in the Earth's magnetosphere

Numerical simulations of particle motion in model magnetic and electric fields allow to study many features of the particle behavior in the Earth's magnetosphere, their precipitation as well as the refilling of radiation belt populations. It was the subject of many works (see, e.g., Delcourt et al., 1992; Li et al., 1998). When the particle motion is adiabatic (i.e., when the magnetic field line curvature radius is much greater than the particle gyroradius and the gyroperiod is much less than the characteristic time of the magnetic field change) the guiding center approximation can be used. When adiabatic conditions are violated it is necessary to compute the full equation of motion, which takes much more computer time, especially for electrons. A number of features of particle motion can be studied with fairly simple magnetic and electric field models. However, in this study, a close comparison of simulation results with specific DOK-2 datasets requires us to use models that are as realistic as possible and especially that can reproduce the state of the magnetosphere for the observation period considered. For ions in the DOK-2 energy range (50–800 keV), traveling in the regions of outer magnetosphere close to its boundaries as well as in

the near plasma sheet region, the full particle trajectory calculation must be used.

Initially, we applied a program code developed by Delcourt to study the circulation of ions with relatively low energies (up to a few tens of kiloelectrovolt) (Delcourt et al., 1992), using the magnetic field model of Tsyganenko (1989, 1990) and the electric field model of Volland (1978). The code allowed working either in guiding center (gc) or in full particle (p) mode or in combined mode: gc-mode at $R<R_c$ and p-mode at $R>R_c+R_E$. We used $R_c=7R_E$. Although this code uses a dipole approximation for the internal magnetic field and assumes the solar wind direction to be perpendicular to the dipole axis (i.e., zero tilt), it allowed us to investigate how simulation results depend on the geomagnetic activity (via K_p-index), on the initial conditions (particle energy, pitch angle, gyrophase) and on the electric field. It was found that

- simulation results are not very sensitive to initial gyrophase and pitch angle,
- for ions with $E>100$ keV it is necessary to use the p-mode, because adiabaticity conditions are not fulfilled at $R>7R_E$ especially in the night side of the outer magnetosphere. The calculation time stay here quite acceptable. For electrons the motion remains adiabatic even for $E=300$ keV and gc-mode or combined gc + p-mode can be used to decrease the computation time,
- the program runs with and without the electric field (for polar cap potential drop ~ 50 kV) showed that by $E>100$ keV the elimination of the electric field do not lead to any serious errors,
- The K_p index—the only parameter in Tsyganenko-89 model (6 levels), which determines also the polar cap potential drop used for calculation of the electric field, has a considerable influence on simulation results, especially in the nightside magnetosphere.

Requirements to a model accuracy are limited by an accuracy of the final result (i.e., the test particles position at the time $T0$). The latter depends on the uncertainty of the determination of $T0$, which was 10–30 s. Because particles may significantly travel during such time intervals, it is preferable to track the position of the ionospheric foot ($MLAT_F$ and MLT_F) of the magnetic field line on which the particle is located at $T=T0$. Numerical simulations show that a 30 s change in $T0$ value lead to the change in the magnetic field line foot parameters at $T=T0$ shown in Table 1.

Our work with T89 model showed that it is important to use more realistic magnetic field models taking into account more parameters, in particular, the solar wind pressure and the interplanetary magnetic field. The code was accordingly modified

- to include the latest IGRF (internal) and Tsyganenko-96_01 (external) magnetic field models with explicit tilt,
- to treat with relativistic particles and, in particular, with energetic electrons.

Table 1
Changes in magnetic field line foot coordinates corresponding to the 30 s change in $T0$

Particle	Energy (keV)	$\Delta MLAT_F$ (deg)	ΔMLT_F (h)
Proton	245	1.17	1.23
Electron	328	0.75	0.69
Proton	45	0.15	0.12
Electron	56	0.18	0.12

As an adequate electric field for any given tilt is not implemented yet, we considered mainly particles with $E>100$ keV, for which the electric field can be neglected.

4. Determination of FDS particle injection position

Fig. 2 shows an example of ion and electron trajectory simulations for the FDS event on February 13, 1997. The calculations were made in p-mode for proton and in combined gc + p mode for electron. In both cases we used the IGRF (internal) and Tsyganenko-96_01 (external) magnetic field models Tsyganenko (1995, 1996) without electric field. The model parameters were: $P_{SW}=2$ nP, $BY_{IMF}=1$ nT, $BZ_{IMF}=2$ nT, DST = −16 nT. The resulting field line parameters for $T=T0$ are given in lower panels.

We have made such calculations for test protons and electrons with different energies for two FDS events in the auroral zone on February 13, and June 28, 1997 (both with Interball-2 data). Fig. 3 shows the results of these calculations using polar ($MLT_F, MLAT_F$) coordinates. Great asterisks correspond to the projection of the first UVI brightening spots (Polar) close to $T0$. The brightening is caused by precipitating energetic electrons moving with low pitch angles from the acceleration site in the plasma sheet along the magnetic field lines. We cannot expect a good correspondence of these projection to the calculated drift start positions because the acceleration site may not coincide with these positions and steady magnetic field model predictions for such far and unstable region as plasma sheet cannot be accurate. Nevertheless it can be seen that, in both cases the injection positions and UVI brightening projections occur in the same evening–midnight sector. Note that the spread in injection positions for the different species and energies is comparable with our initial estimate based on the spectral line width. Our simulations with T89 + dipole model with Volland electric field model showed that final position for 45 keV ions become closer to that of high-energy ions (the electric field increases the drift velocity in this case). So the spread will possibly

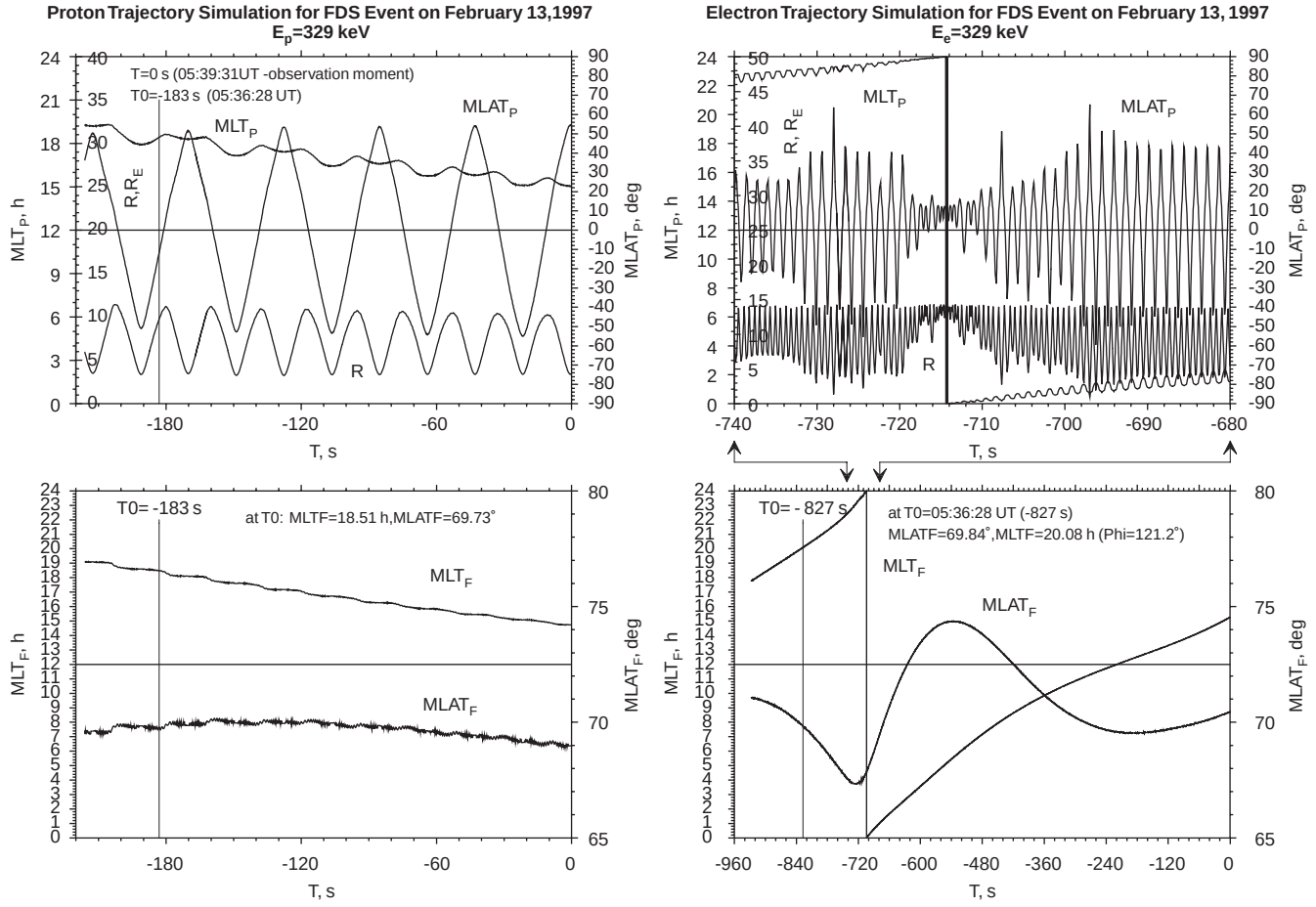

Fig. 2. Results of proton and electron trajectory simulation for the FDS event on February 13, 1997. Upper panels correspond to test particle spherical coordinates (R, $\mathrm{MLT_P}$, $\mathrm{MLAT_P}$), lower ones—to corresponding magnetic field line foot in the ionosphere ($\mathrm{MLT_F}$, $\mathrm{MLAT_F}$). The upper panel for electron gives only part of the trajectory near midnight $\mathrm{MLT_P}$. The time $T = 0$ corresponds to the observation time and $T0$—to the injection time determined by the experiment data analysis.

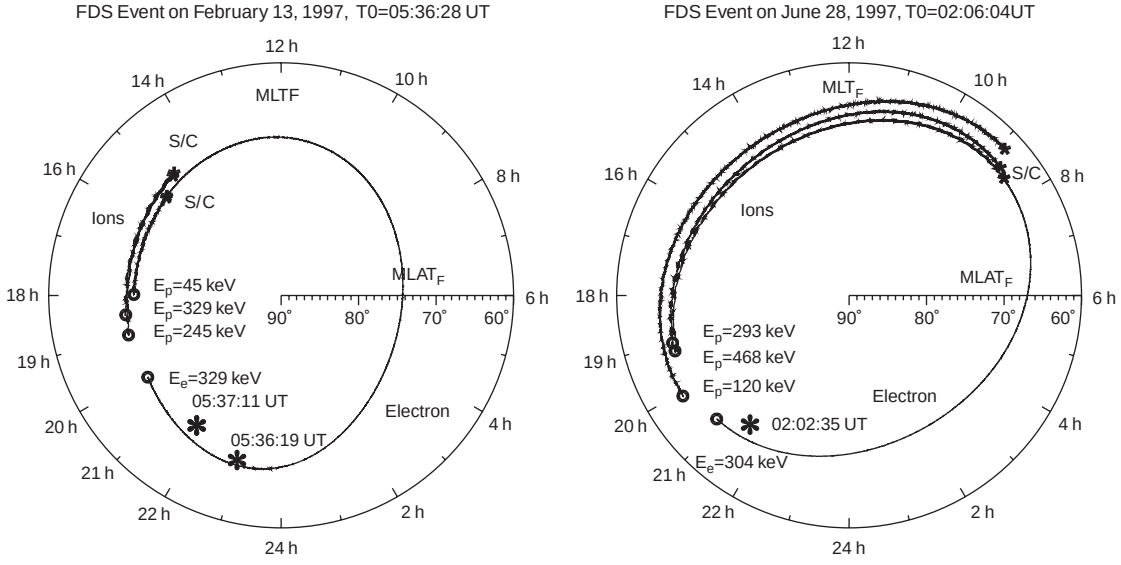

Fig. 3. Simulation results for two FDS events. The spacecraft positions are indicated by small asterisks, the test particle position at $T = T0$ by circles. Great asterisks show the projections of the first UVI brightening spots (Polar) close to $T0$.

decrease also in the T96_01 + IGRF model with addition of the adequate electric field. Certainly much more events should be analyzed before some definite conclusions can be made.

5. Comparison of computed drift periods with the observations

It was shown in Sections 3 and 4 that particle trajectory simulations in T96_01 + IGRF magnetic field model may give selfconsistent results for the source position for different species and different energies. But it was done for time intervals lower than the drift period. The applicability of the method and magnetic field models used to much greater time intervals must be tested. It was done for the FDS event on September 18, 1996 in which we observed ions, which have made several turns around the Earth. Fig. 4 shows an example of q/E vs. time plot for this event. The straight-line fittings for three dispersion structures point to the same $T0$ value: 21:02:17 UT. This plot allows to find drift period values for different q/E. The validity of magnetic field models is generally established through the comparison with magnetic field datasets from satellites located at different points and at different times. The comparison of drift periods identified in FDS events with results of particle trajectory computations open up the possibility to check and compare different magnetic field models not at specific points but in the whole outer magnetosphere on fairly short time scales

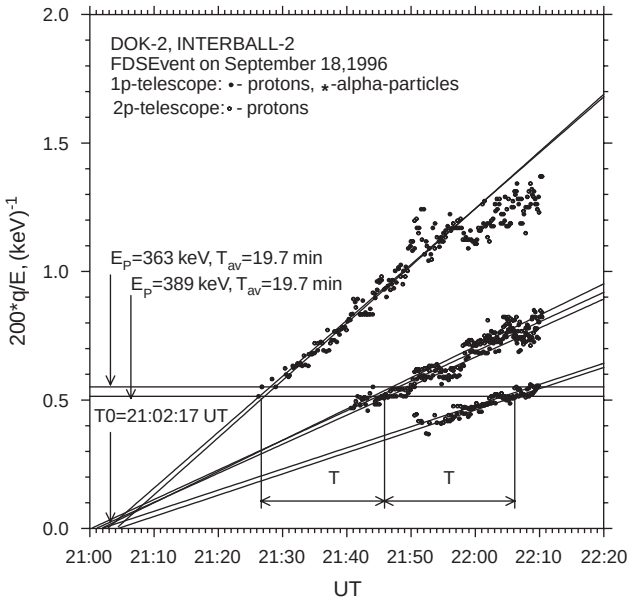

Fig. 4. Drift period determination from the analysis of FDS event on September 18, 1996 corresponding to two full turns of ions around the Earth.

($\Delta T \sim 30$–40 min), hence in about the same magnetospheric state.

Fig. 5 shows the results of such calculations for two protons with close energies during 4–5 successive turns around the Earth for two magnetic field models: T89 + dipole and T96_01 + IGRF. The asterisks show the spacecraft coordinates when these energies were observed. It is apparent from Fig. 5 that, in both magnetic field models, the computed drift periods are smaller than the observed ones. The average ratios T_{com}/T_{obs} were: 0.62 for T89 + dipole and 0.84 for T96_01 + IGRF models. It means that, for the drift shells considered ($L = 10$–12), the average $\nabla B/B$ ratio that controls the drift velocity is too large in both models especially in the first one. Both models give bad predictions of proton trajectories for time intervals greater than the drift period in this region close to the magnetosphere boundary. The results occurred here very sensitive to small changes in magnetic field model and initial test particle parameters: energies, pitch angles, start positions. For this reason we did not make attempts to find a source position for September 18, 1996 event because the time interval between $T0$ and the first observation of FDS ions exceeds here the drift period. The simulations explain also some peculiarities of the particle drift. Indeed, it can be seen in Fig. 5 that, in some turns, particles reaching the noon sector do not bounce around the magnetic equator but near local field minima at MLAT = 25–30°(drift shell branching, see Shabansky (1968); Shabansky and Antonova (1968); Shabansky (1971)). Fig. 6 shows a part of 389 keV proton trajectory including the drift shell branching region in Cartesian SM-coordinates. Our simulations show that particles are delayed when they experience such bounce motion at mid-latitudes and their drift period accordingly increases. It may explain possibly periodic deviations of points from the straight line for the second FDS in Fig. 4.

6. Summary

1. The simulations performed allow, in principle, to calculate the FDS particle injection position. The spread in injection locations for different species and energies is about 1–1.5 h MLT and 0.2–0.3°MLAT in agreement with estimations from the spectral line width analysis. For the two FDS events analyzed the injection region was found in the evening–midnight sector in the vicinity of projections of early UVI brightening spots in the aurora.

2. The magnetic field models used lead to inaccurate results for time scales that exceed the drift period. In comparison with our observations, they yield faster particle drifts around the Earth, especially the T89 + dipole combination.

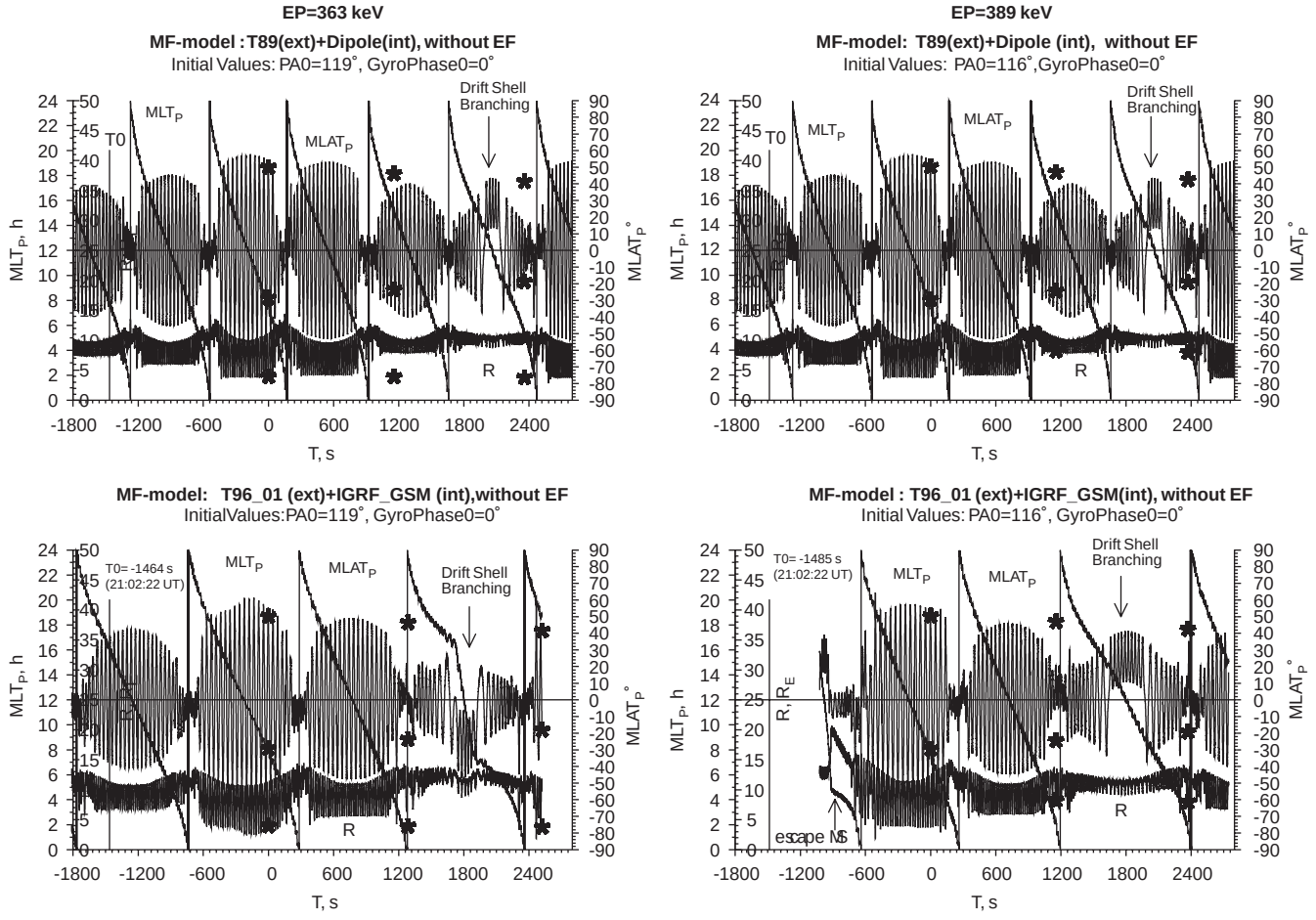

Fig. 5. Simulation of proton trajectories for $E = 363$ keV (left) and $E = 389$ keV (right), using two magnetic field models. T is the time from the first observation of ions with this energy. The parameters used for magnetic field models: $K_p = 2.7$ (T89 + dipole), $P_{sw} = 1.2$ nP, DST $= -27$ nT, $BY_{imf} = 1.5$ nT, $BZ_{imf} = -1$ nT (T96_01 + IGRF). Asterisks show the spacecraft coordinates at all three observation moments.

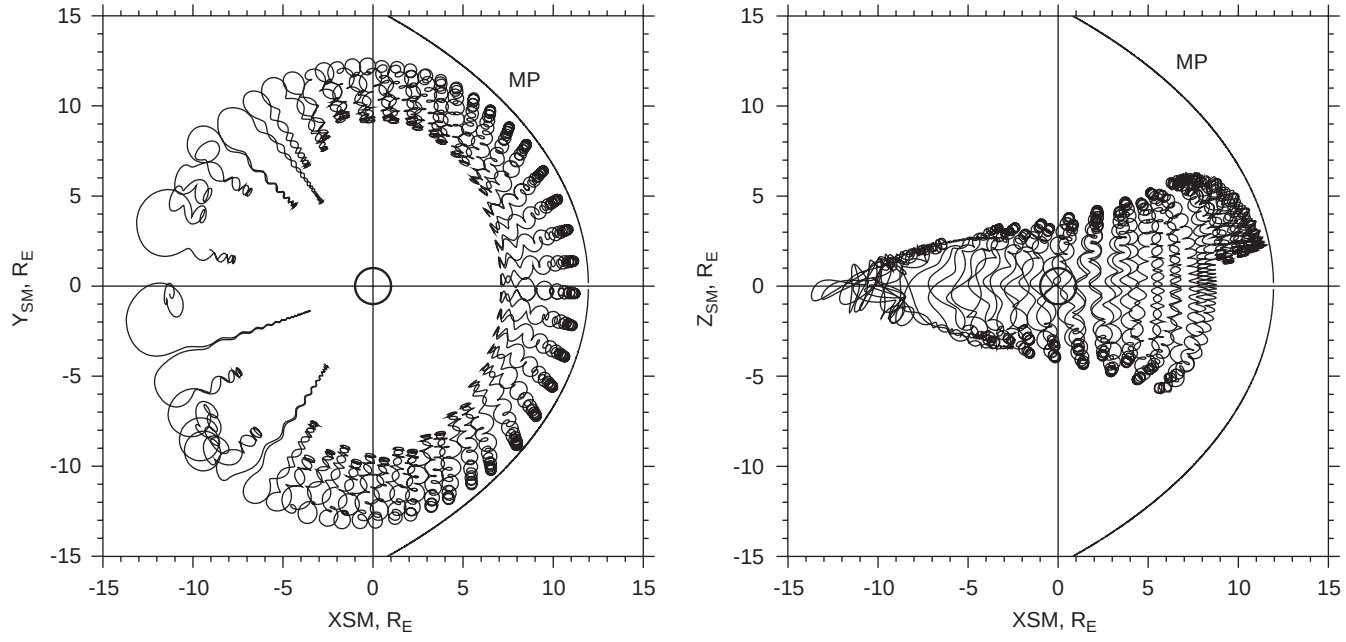

Fig. 6. Proton transition through the north drift shell branching region for $E = 389$ keV (September 18, 1996 event). Left panel: X–Y trajectory projection, right panel: X–Z trajectory projection (T96_01 + IGRF magnetic field model).

Acknowledgements

The work was supported by RFFI Grants 02-02-16309 and 02-02-17160. The authors thank Dr. A.E. Antonova for his useful comments.

References

Anderson, B.J., Takahashi, K., 2000. Pitch angle dispersion of ion injections. J. Geophys. Res. 105, 18709–18727.

Belian, R.D., Baker, D.N., Hones Jr., E.W., Higbie, R.P., 1984. High energy proton drift echoes: multiple peak structures. J. Geophys. Res. 89, 9101–9106.

Birn, J., Thomsen, M.F., Borovsky, J.E., Reeves, G.D., McComas, D.J., Belian, R.D., 1996. Plasma and energetic particle properties of dispersionless substorm injections at geosynchronous orbit. Substorms 3, ESA SP-339, 321–326.

Delcourt, D., Moore, T.E., Sauvaud, J.-A., Chappell, C.D., 1992. Nonadiabatic transport features in the outer cusp region. J. Geophys. Res. 97, 16833–16842.

Karra, M., Fritz, T.A., 1999. Energy dispersion features in vicinity of the cusp. Geophys. Res. Lett. 26, 3553–3556.

Li, X., Baker, D.N., Temerin, M., Reeves, G.D., Belian, R.D., 1998. Simulation of dispersionless injections and drift echoes of energetic electrons associated with substorms. Geophys. Res. Lett. 25, 3763–3766.

Lutsenko, V.N., Kudela, K., Sarris, E.T., 1998. The DOK-2 experiment to study energetic particles by the tail and auroral probe satellites in the Interball project. Cosmic Res. 36, 98–107.

Lutsenko, V.N., Grechko, T.V., Kudela, K., 2000. Interball-2 and -1 observations of energy dispersion events in Auroral zone for 30–500 keV ions and electrons. Substorms 5, ESA SP-443, 519–522.

Lutsenko, V.N., Gretchko, T.V., Kobelev, A.V., Kudela, K., 2002. Dispersion structures in the energetic ion and electron spectra in the Auroral regions: their nature, properties and implication. Adv. Space Res. 30, 1787–1793.

McIlwain, C.E., 1974. Substorm injection boundaries. In: McCormac, B.M., Reidel, D. (Eds.), Magnetospheric Physics. Dordrecht-Holland, pp. 143–154.

Shabansky, V.P., 1968. Magnetospheric processes and related phenomena. Space Sci. Rev. 8, 366–454.

Shabansky, V.P., 1971. Some processes in the magnetosphere. Space Sci. Rev. 12, 299–418.

Shabansky, V.P., Antonova, A.E., 1968. Topology of particle drift shells in the Earth's magnetosphere. Geomagn. Aeronomy 8, 993–997.

Tsyganenko, N.A., 1989. A magnetospheric magnetic field model with a warped tail current sheet. Planet. Space Sci. 37, 5–20.

Tsyganenko, N.A., 1990. Quantitative models of the magnetospheric magnetic-field—methods and results—a review. Space Sci. Rev. 54, 75–186.

Tsyganenko, N.A., 1995. Modeling the Earth's magnetospheric magnetic field confined within a realistic magnetopause. J. Geophys. Res. 100, 5599.

Tsyganenko, N.A., 1996. Effects of the solar wind conditions on the global magnetospheric configuration as deduced from data-based field models. European Space Agency Publication. ESA SP-389, p. 181.

Volland, H., 1978. A model of the magnetospheric electric convection field. J. Geophys. Res. 83, 2695–2699.